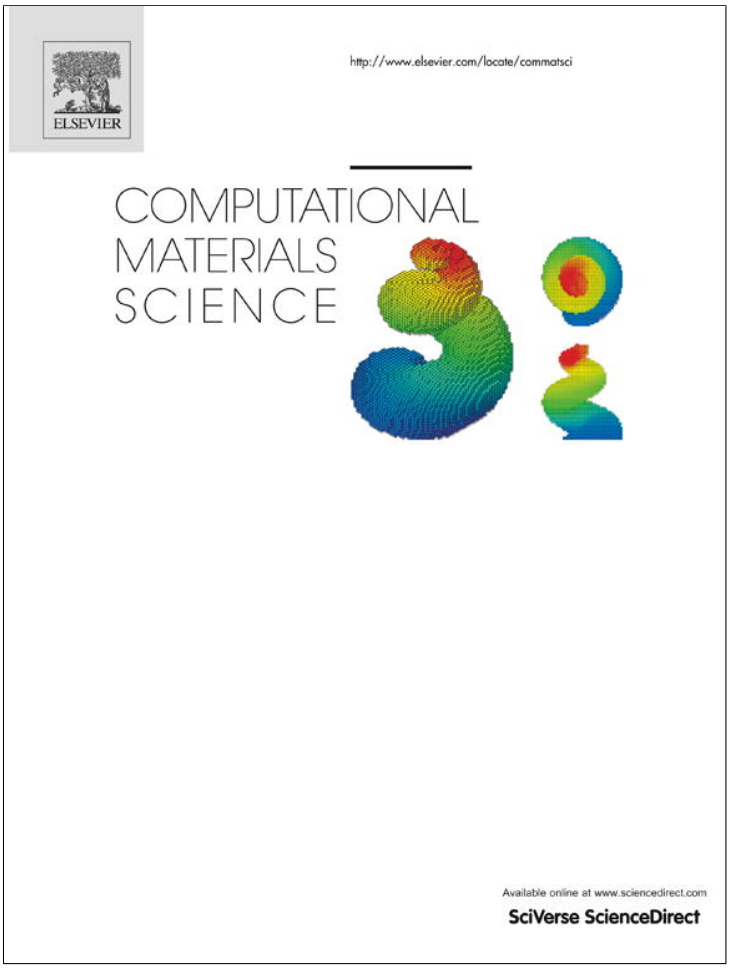

(This is a sample cover image for this issue. The actual cover is not yet available at this time.)

Computational Materials Science 70 (2013) 8–12

Contents lists available at SciVerse ScienceDirect

Computational Materials Science

journal homepage: www.elsevier.com/locate/commatsci

Molecular dynamics simulations for thermal transport behavior of InAs nanotubes: A role of symmetry

Suin Yi, In Kim, Tod A. Pascal, Yousung Jung *

Graduate School of EEWS (WCU), Korea Advanced Institute of Science and Technology (KAIST), Daejeon 305-701, Republic of Korea

ARTICLE INFO

Article history:
Received 27 August 2012
Received in revised form 21 October 2012
Accepted 17 December 2012

Keywords:
Thermoelectrics
Indium arsenide
Nanowire
Nanotube
Molecular dynamics
Thermal conductivity

ABSTRACT

Molecular dynamics simulations for the indium arsenide (InAs) nanowires and nanotubes are performed to understand the improved (decreased) thermal transport behavior in nanostructured systems. The InAs nanotubes have a significantly reduced heat flow as compared to the nanowire analogue due to the increased surface area to volume effect. A 53% reduction in thermal conductivity was observed with a 17% reduction in the nanowire cross sectional area. Local heat current analysis shows that the interior atoms being removed in nanotubes have the largest local heat current contribution, thereby punching a hole in the middle leading to the largest reduction in thermal conductivity of the material. We then find that the broken symmetry can lower the thermal conductivity even further. As a result, a sweet spot for the lowest thermal conductivity for nanotubes is found at the nearest displacement of the hole from the center due to the two opposing factors: highest local heat currents for the innermost atoms and the effect of broken symmetry. We expect that this new physical mechanism of heat transport in InAs nanotubes can be generalized to other thermoelectric materials such as silicon nanowires and nanotubes to reduce a lattice thermal conductivity even further.

1. Introduction

Thermoelectric materials (TE) directly convert heat energy to electrical energy without any moving parts that can cause problems in other electricity generators in the long term. The figure of merit of the TE material can be assessed as $ZT = S^2\frac{\sigma T}{\kappa}$, where S, σ, κ, and T are Seebeck coefficient, electric conductivity, thermal conductivity, and temperature, respectively. Unfortunately, parameters that determine ZT are inter-dependent one another, i.e., changing one parameter to improve ZT sometimes affects the other parameters adversely, and ZT has been around 1 for over half a century [1]. Since the work of Hicks and Dresselhaus which suggested that using low dimensional structure can increase the electrical properties far beyond that of bulk material, various nanostructures have been designed and studied for TE applications [2]. Many of the improvements however were due to a reduction of the thermal conductivity rather than the increase of electronic properties [3]. The silicon nanowire is one of such materials.

Bulk silicon, with ZT = 0.01 [4] and $\kappa \sim 150$ W/mK [5] at room temperature, shows a poor performance as a thermoelectric material, but silicon nanowires can have a reduced lattice thermal conductivity as much as two orders of magnitude smaller compared to the bulk silicon due to an increased phonon scattering at the confining walls [6,7]. Significant further reduction of the thermal conductivity of silicon was shown both theoretically and experimentally by increasing the surface area to volume ratio (SVR) in the form of nanotubes or nanoporous materials [8–10]. A number of theoretical studies have also been proposed for the silicon and germanium IV semiconductors to reduce thermal conductivity [11–20], including the Si/Ge core–shell nanowires that showed 75% decrease in thermal conductivity at room temperature compared to an uncoated Si nanowire [18]. Other group III–V semiconductors such as InAs and InSb alloys have also been considered due to their high electron mobility arising from light effective electron masses [21,22]. The nanowire forms of InSb and InAs have been proposed theoretically as a possible efficient thermoelectric material [23–25] and semiconductor alloys containing In, Ga, and As have shown ZT = 0.9 at 800 K [26–28].

In this work, we consider various structures of InAs nanotubes (InAsNTs) and report a significant reduction of the lattice thermal conductivity as compared to InAs nanowires (InAsNWs) by 53%, by a 17% reduction in the nanowire cross section. In particular, we find that changing the nanotube geometry and symmetry while maintaining the total SVR the same can lower the thermal conductivity even further, a point that was neglected in previous studies [8,9,11]. Assuming that the electrical properties are not negatively affected, the latter reduction of thermal conductivity would yield an improved thermoelectric performance.

* Corresponding author.
E-mail address: ysjn@kaist.ac.kr (Y. Jung).

0927-0256/$ - see front matter © 2013 Elsevier B.V. All rights reserved.
http://dx.doi.org/10.1016/j.commatsci.2012.12.024

2. Methods

We used non-equilibrium molecular dynamics (MD) simulation, a so-called direct method, to measure the thermal conductivity of InAsNWs and InAsNTs [29]. Because InAs is not a homogeneous system, the Green–Kubo method, another method to calculate thermal conductivity, requires long simulation time to use low pass filters [30]. Hence we used the direct method for this binary alloy system [25]. We set the [1 1 1] direction of InAs zinc-blend structure as a longitudinal *z*-axis of InAsNWs and InAsNTs. Fig. 1 shows cross sectional views of the InAsNWs and InAsNTs with various hole positions. The InAsNW is composed of a single row of atoms surrounded by *N* layers of hexagonal group of atoms. InAsNTs are then modeled by deleting the central row as well as the surrounding *M* hexagonal layers of atoms ($M < N$) as shown in Fig. 1. We have considered $M = 1$ and 3 in this study. In a notation (N, M, D), D denotes the displacement of the hole with respect to the center. In other words, for the hole located at the center of the nanotube, $D = 0$, and for the hole that is displaced by one atomic position, $D = 1$ as in Fig. 1. In order to prevent the drift of nanowires and nanotubes, the two outermost surface layers of hexagonal cylinders shown as grey were fixed for InAsNWs, and for the case InAsNTs, both the two innermost and outer surface atoms were fixed [25]. These frozen surface conditions have been previously applied to investigate thermal transport in nanowires with unsaturated surface atoms, which confirmed that the results based on the free and frozen surface approximations show a reasonable agreement [31,32]. These frozen layers can also mimic the experimental conditions of NWs and NTs that are covered with amorphous coating [25] and since they are frozen, they do not contribute to the calculation of thermal conductivity and hence not counted in determining *N* and *M* in Fig. 1. We used the 150 nm long InAsNWs and InAsNTs in our simulations. A recent MD study reported that the thermal conductivity could diverge depending on the length of a unit cell [33], and we observed a similar behavior in this work when increasing the length of InAsNWs systematically from 50 to 400 nm. Nevertheless, a comparison of the relative thermal conductivity of NTs and NWs for a fixed length is expected to be valid [18]. We used the Abell–Tersoff force field (FF) parameters for indium and arsenic atoms [34,35]. Initially, the entire structure

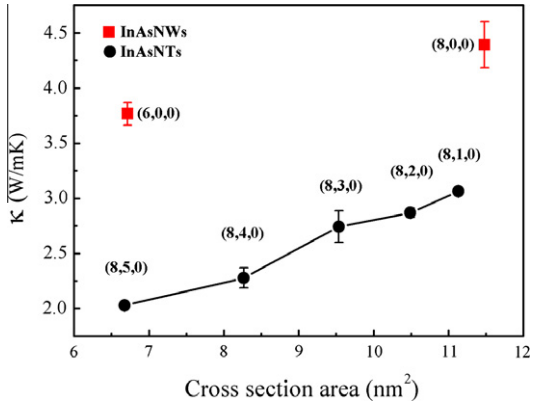

Fig. 2. The calculated thermal conductivities of two InAsNWs with $(N,M,D) = (6,0,0)$, $(8,0,0)$, and five InAsNTs with $(N,M,D) = (8,1,0)$, $(8,2,0)$, $(8,3,0)$, $(8,4,0)$, and $(8,5,0)$.

was placed in a Langevin heat bath of 300 K to reach an equilibrium. Then, temperature gradient was established in the NVE ensemble by scaling the velocities of atoms in the heat source and sink, i.e., 3 layers in each region, to yield the net heat flow of 2.5–5 meV/ps. Within 2 ns, a steady state was reached. The 150 nm was divided into 25 segments for analysis and the temperature of each segment was averaged over 8 ns to determine the temperature gradient after steady state. Considering the non-linear effect near the heat source and sink, the nine segments in the middle were taken for extracting the temperature gradient [29]. Thermal conductivity was calculated by Fourier's law. LAMMPS package [36] was used to perform all MD simulations.

3. Results and discussions

The calculated thermal conductivities of two InAsNWs (6,0,0) and (8,0,0), and five InAsNTs with (N,M,D) = (8,1,0), (8,2,0), (8,3,0), (8,4,0), and (8,5,0) are shown in Fig. 2. By punching a tiny hole of 0.3576 nm^2, from (8,0,0) to (8,1,0), the thermal conductivity is reduced by 33%. Since we used the fixed boundary condition for inner most layers in MD simulations of InAsNTs, it is important

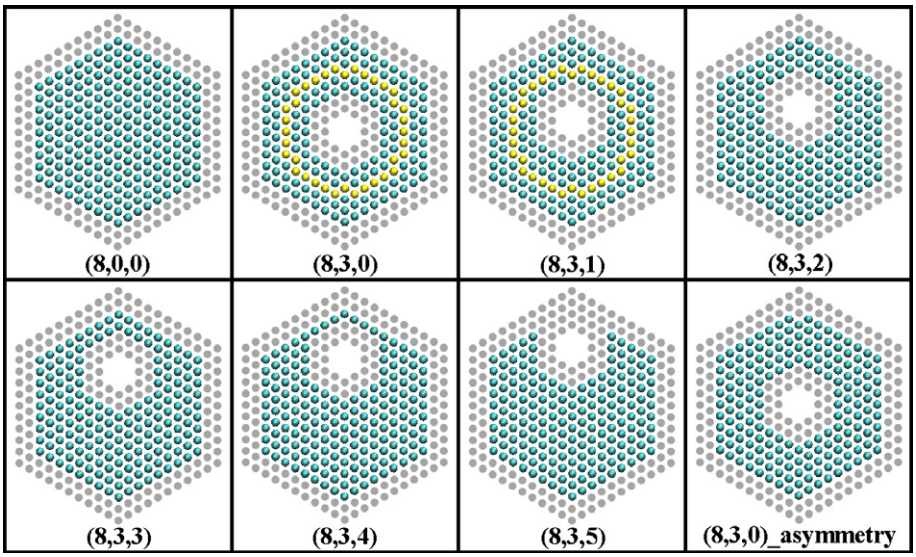

Fig. 1. Cross sectional view of various nanostructures (diameter ≈ 4 nm, length = 150 nm) studied in this work. The (N,M,D) notations are explained in the main text. The two outermost and innermost layers shown in grey are fixed (frozen), and thus not included in the calculation of thermal conductivity. The atoms in yellow for (8,3,0) and (8,3,1) are those that were used to calculate the angular distribution of the local heat current in Fig. 5b. (For interpretation of the references to color in this figure legend, the reader is referred to the web version of this article.)

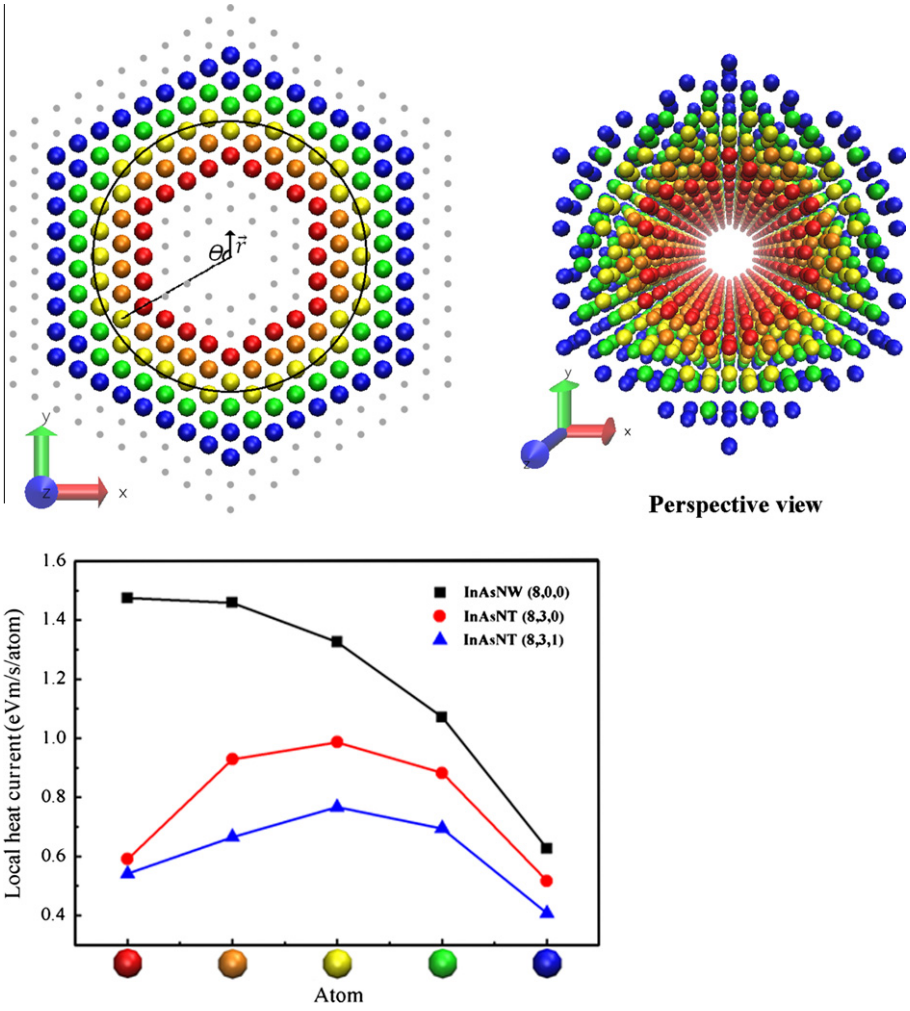

Fig. 3. (a) A schematic that shows the color codes of the atomic positions in a radial direction: from inner to outer, we use red, orange, yellow, green, and blue. (b) Radial distribution of the local heat current for InAsNW (8,0,0), InAsNT (8,3,0) and (8,3,1) for the five radial positions. (For interpretation of the references to color in this figure legend, the reader is referred to the web version of this article.)

to verify that the observed reduction in thermal conductivity is due to the "hole" rather than the particular boundary condition employed. Therefore, we performed additional calculations with free inner layers for (8,1,0). We find that a large reduction in thermal conductivity is still observed with the free inner layers, validating the frozen inner layer approach. In fact, the computed thermal conductivity of nanotubes with free inner layers (2.55 W/mK) was even lower by 14% than that calculated with fixed inner layers. A linear decrease in thermal conductivity is observed as a function of hole size, which is consistent with the results for silicon nanotubes [9] since a higher SVR induces more phonon localization at the surface. For example, a large 50% reduction in thermal conductivity for (8,5,0) as compared to (6,0,0) with comparable cross sectional area (6.715 nm^2 vs. 6.675 nm^2, respectively) arises from the increased surface area to volume ratio of the nanotube.

In order to analyze which local area is mainly responsible for the reduced thermal conductivity, the local heat current analysis was performed [29] along the z-direction with a segment of $\Delta z = 10$ nm:

$$\vec{J} = \frac{d}{dt} z(t) E(t)$$

where $z(t)$ is atom's position vector and $E(t)$ is the energy of atom at a specific time t. Due to a large fluctuation of the heat current originated from the heterogeneous structural character [30], the local heat current values were averaged for the time duration of 10 ns. Fig. 3a shows a local heat current for the five concentric regions along the radial direction. Not surprisingly, in the case of a nanowire (8,0,0), the surface atoms (blue) show a lower local heat current than the atoms inside and color-coded with red as much as 60% due to a phonon localization at the surface [8,9]. For this nanowire, we also observe the convergence of the local heat current to a bulk behavior at the third to fourth layers from the surface. For a nanotube (8,3,0), however, newly created surface by an introduction of the hole induces more phonons to be localized at the internal surface and reduces thermal conductivity further, consistent with the results for the silicon nanotubes [9]. The difference between NW and NT decreases as we move from inside to outside, but it is interesting that there still exists some noticeable difference in the local heat current for the outermost surface layer depending on the presence or absence of the hole in the middle.

We calculated the vibrational density of states (VDOS) to understand the changes in the behavior of phonons in the presence of a hole by Fourier transform of the velocity auto correlation function. We used the correlation time to be 6.144 ps. In Fig. 4, the inner and outer surfaces of InAsNW (8,0,0) and InAsNT (8,3,0) are analyzed separately. A significant depression in VDOS is exhibited at the inner surface of NT both in low frequency (0–3.5 THz) and high frequency (~6.5 THz) regions as compared to the atoms in the same position of NW. For the outer surface in Fig. 4b, however, there is

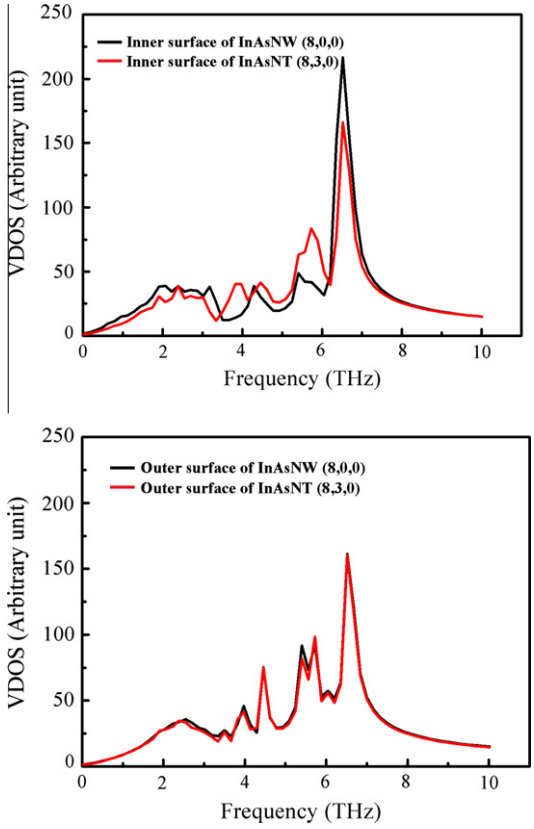

Fig. 4. Local vibrational density of states of InAsNW and InAsNT at (a) the inner surface and (b) the outer surface. The "inner surface" of nanowire is defined as atoms with the same atomic positions as the inner surface of a hole in nanotube.

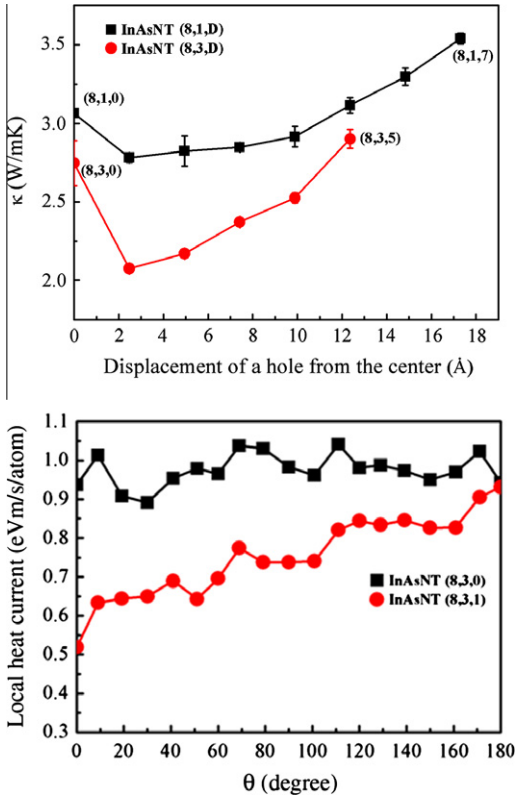

Fig. 5. (a) The thermal conductivity of InAsNT $(8,1,D)$ and $(8,3,D)$ as a function of the displacement of a hole. The cross-sectional areas for all $(8,1,D)$ with $D = 1$–7 considered here are the same since the hole is still confined within the boundary of the nanotubes. Similarly, the cross-sectional areas in all $(8,3,D)$ cases considered here are the same. (b) Concentric angular distribution of the local heat current for InAsNT $(8,3,0)$ and $(8,3,1)$ for the atoms colored in yellow in Figs. 1 and 3a. The reference ($\theta = 0$) is the direction along the displacement vector r as in Fig. 3a.

almost no difference in VDOS for NT and NW despite the introduction of a hole in NT. These VDOS results support the conclusion of Fig. 3 that the new surface created by the hole is responsible for the decreased heat current of the nanotube. Several new peaks at intermediate frequencies around 3.8 THz and 5.8 THz are similar to Hu et al. for the silicon–germanium core/shell nanowire structures [18].

We investigated the effect of a hole position on the thermal conductivity of a nanotube. The results shown in Fig. 5a for $(8,1,D)$ nanotubes with various hole displacements are rather surprising since nearly all previous works attributed the reduced thermal conductivity to a simple surface area to volume ratio [8,9,11]. However we observe that the thermal conductivity can vary as much as 30% for nanotubes with 3.81 nm outer-diameter and 9.47 nm^2 cross sectional area depending on the position of a hole while they have the same surface area to volume ratio. In particular, we find that there is a sweet spot for the lowest thermal conductivity depending on the position of the hole where the minimum occurs at the nearest displacement from the center. This trend can be explained by two factors: the local heat current of the interior atoms being deleted and the symmetry of the nanotube. On the basis of Fig. 3b, removing the innermost atoms with the highest heat current would have the biggest effect on reducing the total heat conductivity, while, with the fixed SVR, deleting the outermost atoms of NW with the lowest heat current would yield the least effect on the thermal conductivity. In this regard, the NT with a hole in the exact center, such as in $(8,1,0)$ or $(8,3,0)$, would have the lowest thermal conductivity. However, there is a symmetry effect that makes $(8,3,1)$ rather than $(8,3,0)$ have the largest decrease in heat conductivity as described below.

To examine the symmetry effect on the lowering of thermal conductivity, we have plotted in Fig. 5b the angular distribution of the local heat current for the two hole positions, center of NT and off-centered by one atomic position. Interestingly, we observe a reduced heat current throughout the entire cross section of the displaced nanotube $(8,3,1)$ compared to that of $(8,3,0)$, including those atoms with $\theta > 90°$ that move away from (and hence experience a diminished effect of) the inner surface after the displacement of a hole (see yellow atoms in Fig. 1). This is counter-intuitive since one would expect that the latter yellow atoms after the displacement would feel lesser surface effects and become more bulk-like after the displacement of the hole with the increased heat current relative to the pre-displacement. However, our simulations and analysis yield the opposite results, meaning that, in addition to the simple surface effects widely discussed, there must be an additional effect due to the breaking of central symmetry in lowering the thermal conductivity. Although we compared the VDOS of InAsNTs $(8,3,0)$ and $(8,3,1)$, we did not find any noticeable difference in VDOS before and after breaking symmetry.

Thus, we considered several different models to explore this symmetry effect where 1–3 row of atoms at a corner were removed or added as shown in Fig. 6 and Table 1 as different ways of breaking symmetry. The calculated thermal conductivities are shown in Table 1. The model '1-corner removed' has the SVR almost the same as the original NT with the hole at the center, but we find a significant reduction in thermal conductivity by 15% by removing a row at a corner. Interestingly, in a '1-corner added' model, we find that the thermal conductivity further decreases despite the reduced SVR. For the model '2-corner added' or '3-corner added', which breaks a mirror symmetry compared with the model '1-corner added', the thermal conductivity decreases again despite

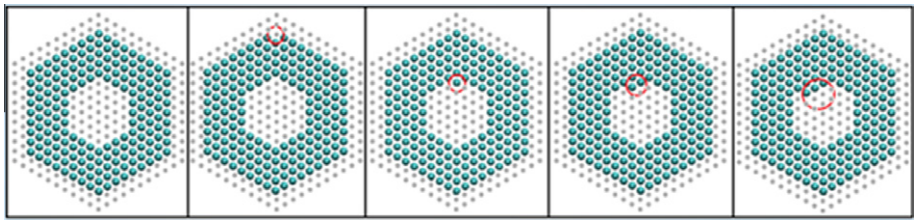

Fig. 6. Various nanotube configurations (cross-sectional view) with broken symmetry while maintaining the surface and cross-sectional areas nearly the same within 2%.

Table 1
The calculated thermal conductivity for various NT configurations with broken symmetry while maintaining the surface area to volume ratio (SVR) the same within 2%.

Model	(8,3,0)	1-Corner removed	1-Corner added	2-Corner added	3-Corner added
SVR (%)	Reference	100.6	99.5	98.9	98.4
κ (%)	Reference	86.2	88.6	84.8	86.6
κ (W/mK)	2.74	2.36	2.43	2.33	2.38

the reduced SVR. On the basis of these results, the asymmetry effect can be confirmed to play an important role in reducing the thermal transport in the nanotube geometries. We expect that the silicon nanotubes proposed in a previous study by Chen et al. [9], which assumed a simple hole in the center, would also show an enhanced performance with the position of a hole changed for symmetry breaking for decreasing the thermal conductivity even further.

4. Conclusion

We reported using molecular dynamics simulations that InAs nanotubes have a reduced thermal conductivity compared to InAs nanowires by 53% (with a 17% reduction in the nanowire cross section area). In addition to this surface area to volume effect, we find that breaking the symmetry of nanotubes can lower thermal conductivity even further when compared to the nanotubes with the same surface area to volume ratio without symmetry breaking. For a given cross-sectional area in nanotubes, the optimal thermal transport behavior is thus obtained with a smallest displacement of a hole due to the balance between the large local heat current of the interior atoms being deleted and the asymmetry of the nanotube.

Acknowledgments

This work was supported by the WCU program (R31-2008-000-10055-0) and the National Research Foundation of Korea (NRF) grant funded by the Korean Government (NRF-2010-0028718). We would like to thank Jaehoon Kim for helpful discussions.

References

[1] A.J. Minnich, M.S. Dresselhaus, Z.F. Ren, G. Chen, Energy Environ. Sci. 2 (2009) 466–479.
[2] L.D. Hicks, M.S. Dresselhaus, Phys. Rev. B 47 (1993) 16631–16634.
[3] G.J. Snyder, E.S. Toberer, Nature Mater. 7 (2008) 105–114.
[4] D.M. Rowe, CRC Handbook of Thermoelectrics, CRC-Press, Boca Raton, FL, 1995. p. 701.
[5] Y.S. Touloukian, R.W. Powell, C.Y. Ho, P.G. Klemens (Eds.), Thermal Conductivity: Metallic Elements and Alloys, Thermophysical Properties of Matter, vol. 1339, IFI/Plenum, New York, 1970.
[6] A.I. Boukai, Y. Bunimovich, J. Tahil-Kheli, J.K. Yu, W.A. Goddard III, J.R. Heath, Nature 451 (2008) 168–171.
[7] A.I. Hochbaum, R. Chen, R.D. Delgado, W. Liang, E.C. Garnett, M. Najarian, A. Majumdar, P. Yang, Nature 451 (2008) 163–168.
[8] J.H. Lee, J.C. Grossman, J. Reed, G. Galli, Appl. Phys. Lett. 91 (2007) 223110.
[9] J. Chen, G. Zhang, B. Li, Nano Lett. 10 (2010) 3978–3983.
[10] J.K. Yu, S. Mitrovic, D. Tham, J. Varghese, J.R. Heath, Nature Nanotechnol. 5 (2010) 718–721.
[11] J.H. Lee, J.C. Grossman, Appl. Phys. Lett. 95 (2009) 013106.
[12] Z. Wang, N. Mingo, Appl. Phys. Lett. 97 (2010) 101903.
[13] I. Ponomareva, D. Srivastava, M. Menon, Nano Lett. 7 (2007) 1155–1159.
[14] N. Yang, G. Zhang, B. Li, Nano Lett. 8 (2008) 276–280.
[15] T.T.M. Vo, A.J. Williamson, V. Lordi, G. Galli, Nano Lett. 8 (2008) 1111–1114.
[16] J.H. Lee, G.A. Galli, J.C. Grossman, Nano Lett. 8 (2008) 3750–3754.
[17] D. Donadio, G. Galli, Nano Lett. 10 (2010) 847–851.
[18] M. Hu, K.P. Giapis, J.V. Goicochea, X. Zhang, D. Poulikakos, Nano Lett. 11 (2011) 618–623.
[19] J.B. Haskins, A. Kinaci, T. Cagin, Nanotechnology 22 (2011) 155701.
[20] D. Donadio, G. Galli, Phys. Rev. Lett. 102 (2009) 195901.
[21] R. Bowers, R.W. Ure, J.E. Bauerle, A.J. Cornish, J. Appl. Phys. 30 (1959) 930–934.
[22] D.L. Rode, Phys. Rev. B 3 (1971) 3287–3299.
[23] N. Mingo, Appl. Phys. Lett. 84 (2004) 2652–2654.
[24] N. Mingo, D.A. Broido, Phys. Rev. Lett. 93 (2004) 246106.
[25] J. Carrete, R.C. Longo, L.J. Gallego, Nanotechnology 22 (2011) 185704.
[26] J.H. Bahk, Z.B. Bian, M. Zebarjadi, J.M.O. Zide, H. Lu, D. Xu, J.P. Feser, G. Zeng, A. Majumdar, A.C. Gossard, A. Shakouri, J.E. Bowers, Phys. Rev. B 81 (2010) 235209.
[27] J.H. Bahk, G. Zeng, J.M.O. Zide, H. Lu, R. Singh, D. Liang, A.T. Ramu, P. Burke, Z. Bian, A.C. Gossard, A. Shakouri, J.E. Bowers, J. Electron. Mater. 39 (2010) 1125–1132.
[28] J.M.O. Zide, J.H. Bahk, R. Singh, M. Zebarjadi, G. Zeng, H. Lu, J.P. Feser, D. Xu, S.L. Singer, Z.X. Bian, A. Majumdar, J.E. Bowers, A. Shakouri, A.C. Gossard, J. Appl. Phys. 108 (2010) 123702.
[29] P.K. Schelling, S.R. Phillpot, P. Keblinski, Phys. Rev. B 65 (2002) 144306.
[30] J. Che, T. Cagin, W. Deng, W.A. Goddard III, J. Chem. Phys. 113 (2000) 6888–6900.
[31] S.G. Volz, G. Chen, Appl. Phys. Lett. 64 (1999) 2056–2058.
[32] C.J. Gomes, M. Madrid, J.V. Goicochea, C.H.J. Amon, Heat Transfer 123 (2006) 1114–1121.
[33] X. Yang, A.C. To, R. Tian, Nanotechnology 21 (2010) 155704.
[34] T. Hammerschmidt, P. Kratzer, M. Scheffler, Phys. Rev. B 77 (2008) 235303.
[35] T. Hammerschmidt, P. Kratzer, M. Scheffler, Phys. Rev. B 81 (2010) 159905.
[36] S.J. Plimpton, J. Comput. Phys. 117 (1995) 1–42.